

The Chaotic Motion of a Double Pendulum

Carl W. Akerlof
September 26, 2012

The following notes describe the kinematics of the double pendulum. The starting point is a pendulum consisting of two point masses, m_1 and m_2 , suspended by massless wires of length l_1 and l_2 . The treatment of this case can be found at:

<http://scienceworld.wolfram.com/physics/DoublePendulum.html>

For a real system, the equations of motion depend in a more complicated way on the distribution of mass that is essential for modeling the physical pendulum used in this experiment.

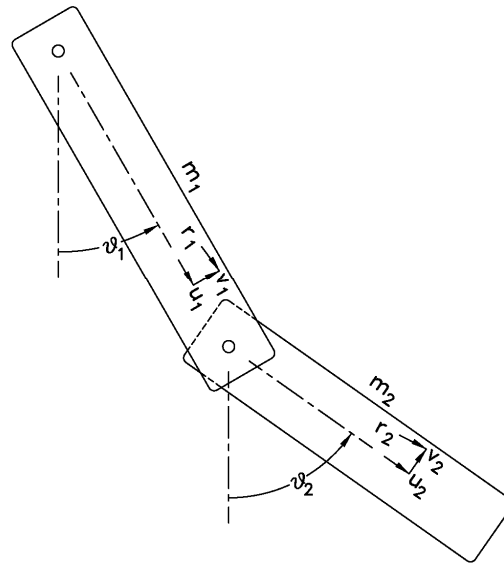
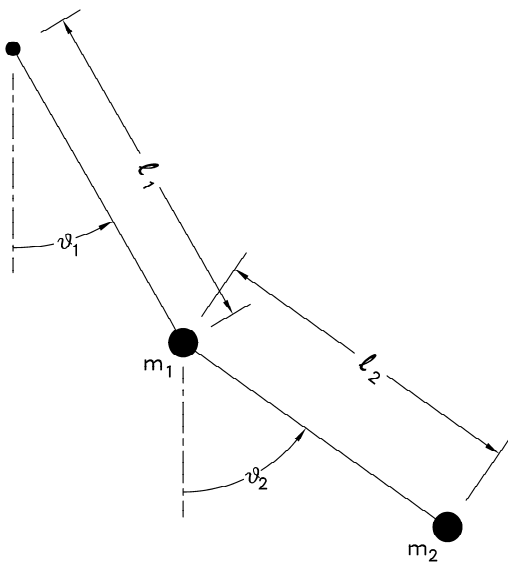


Figure 1. Point mass double pendulum. Figure 2. Extended mass double pendulum.

Double pendulum with point masses:

$$x_1 = l_1 \sin \theta_1$$

$$y_1 = -l_1 \cos \theta_1$$

$$x_2 = l_1 \sin \theta_1 + l_2 \sin \theta_2$$

$$y_2 = -l_1 \cos \theta_1 - l_2 \cos \theta_2$$

$$\dot{x}_1 = l_1 \cos \theta_1 \dot{\theta}_1$$

$$\dot{y}_1 = l_1 \sin \theta_1 \dot{\theta}_1$$

$$\dot{x}_2 = l_1 \cos \theta_1 \dot{\theta}_1 + l_2 \cos \theta_2 \dot{\theta}_2$$

$$\dot{y}_2 = l_1 \sin \theta_1 \dot{\theta}_1 + l_2 \sin \theta_2 \dot{\theta}_2$$

$$\dot{r}_1^2 = l_1^2 \dot{\theta}_1^2$$

$$\dot{r}_2^2 = l_1^2 \dot{\theta}_1^2 + 2l_1 l_2 \cos(\theta_1 - \theta_2) \dot{\theta}_1 \dot{\theta}_2 + l_2^2 \dot{\theta}_2^2$$

Double pendulum with distributed masses:

$$x_1 = u_1 \sin \theta_1 + v_1 \cos \theta_1$$

$$y_1 = -u_1 \cos \theta_1 + v_1 \sin \theta_1$$

$$x_2 = l_1 \sin \theta_1 + u_2 \sin \theta_2 + v_2 \cos \theta_2$$

$$y_2 = -l_1 \cos \theta_1 - u_2 \cos \theta_2 + v_2 \sin \theta_2$$

$$\dot{x}_1 = u_1 \cos \theta_1 \dot{\theta}_1 - v_1 \sin \theta_1 \dot{\theta}_1$$

$$\dot{y}_1 = u_1 \sin \theta_1 \dot{\theta}_1 + v_1 \cos \theta_1 \dot{\theta}_1$$

$$\dot{x}_2 = l_1 \cos \theta_1 \dot{\theta}_1 + u_2 \cos \theta_2 \dot{\theta}_2 - v_2 \sin \theta_2 \dot{\theta}_2$$

$$\dot{y}_2 = l_1 \sin \theta_1 \dot{\theta}_1 + u_2 \sin \theta_2 \dot{\theta}_2 + v_2 \cos \theta_2 \dot{\theta}_2$$

$$\dot{r}_1^2 = r_1^2 \dot{\theta}_1^2 \quad ; \quad r_1^2 = u_1^2 + v_1^2$$

$$\dot{r}_2^2 = l_1^2 \dot{\theta}_1^2 + 2l_1(u_2 \cos(\theta_1 - \theta_2) + v_2 \sin(\theta_1 - \theta_2)) \dot{\theta}_1 \dot{\theta}_2 + (r_2^2) \dot{\theta}_2^2 \quad ; \quad r_2^2 = u_2^2 + v_2^2$$

Assume mirror symmetry: $\langle v_1 \rangle = \langle v_2 \rangle = 0$

$$KE = \frac{1}{2} \left(\langle m_1 \cdot r_1^2 \rangle \dot{\theta}_1^2 + m_2 l_1^2 \dot{\theta}_1^2 + 2 \langle m_2 \cdot u_2 \rangle l_1 \cos(\theta_2 - \theta_1) + \langle m_2 \cdot r_2^2 \rangle \dot{\theta}_2^2 \right)$$

$$PE = - \langle m_1 \cdot u_1 \rangle g \cos \theta_1 - m_2 l_1 g \cos \theta_1 - \langle m_2 \cdot u_2 \rangle g \cos \theta_2$$

Thus, the Lagrangian for the system is:

$$L = T - V = \frac{1}{2} \left(\langle m_1 \cdot r_1^2 \rangle \dot{\theta}_1^2 + m_2 l_1^2 \dot{\theta}_1^2 + 2 \langle m_2 \cdot u_2 \rangle l_1 \cos(\theta_2 - \theta_1) \dot{\theta}_1 \dot{\theta}_2 + \langle m_2 \cdot r_2^2 \rangle \dot{\theta}_2^2 \right) + \langle m_1 \cdot u_1 \rangle g \cos \theta_1 + m_2 l_1 g \cos \theta_1 + \langle m_2 \cdot u_2 \rangle g \cos \theta_2$$

This leads directly to the equations of motion which we shall investigate shortly.

Dynamics of the physical pendulum

The aim of this experiment is to compare the actual dynamical behavior of a real physical pendulum with a mathematical simulation. To this end, we need to characterize the pendulum properties as accurately as possible and incorporate these into the appropriate equations of motion.

One approximation will be involved: the motion will be assumed frictionless. This simplification is driven principally by the lack of any very elegant fundamental theory although it would actually be fairly trivial to incorporate velocity-dependent damping in the dynamical modeling.

The moving parts for the real pendulum are:

- 2 primary axis bearings
- 2 primary arms
- 2 secondary axis bearings
- 2 secondary axis spacers
- 1 secondary axis cap screw
- 1 secondary axis hex nut
- 1 secondary arm

The vendor for this apparatus, *chaoticpendulums.com*, has conveniently provided the dimensions for these parts as shown in Figure 3. Note that all dimensions are in millimeters. The required spatial mass moments can be calculated analytically for each item. The contribution that each one provides to the kinetic and potential energies is given below. For future reference, the distance between the primary and secondary axes is denoted l_1 and equals 173 mm.

Bearing: A bearing facilitates low-friction axial rotation shear while constraining the shaft location. Thus, the inner race of the bearing can be rotating with angular velocity, ω_- , while the outer race is rotating with an angular velocity of ω_+ . To keep the modeling of this component simple, it is assumed that the bearing is homogeneous with a rotation rate at radius, r , that is linearly interpolated by the distances from the inner and outer radii.

Primary axis bearing:

$$KE = \frac{1}{2} \langle m_b \cdot r^2 \rangle_{++} \dot{\theta}_1^2$$

$$PE = 0$$

Secondary axis bearing:

$$KE = \frac{1}{2} \left(m_b l_1^2 \dot{\theta}_1^2 + \langle m_b \cdot r^2 \rangle_{++} \dot{\theta}_1^2 + 2 \langle m_b \cdot r^2 \rangle_{-+} \dot{\theta}_1 \dot{\theta}_2 + \langle m_b \cdot r^2 \rangle_{--} \dot{\theta}_2^2 \right)$$

$$PE = -m_b l_1 g \cos \theta_1$$

Primary arm:

$$KE = \frac{1}{2} \langle m_1 \cdot r^2 \rangle \dot{\theta}_1^2$$

$$PE = -\langle m_1 \cdot u \rangle g \cos \theta_1$$

Secondary axis components:

The cap screw, spacers and hex nut are all constrained to rotate rigidly with the secondary arm.

$$KE = \frac{1}{2} \left(\langle m_c \cdot r^2 \rangle + 2 \langle m_s \cdot r^2 \rangle + \langle m_n \cdot r^2 \rangle \right) \dot{\theta}_2^2$$

$$PE = -(m_c + 2 m_s + m_n) l_1 g \cos \theta_1$$

Secondary arm:

$$KE = \frac{1}{2} \left(m_2 l_1^2 \dot{\theta}_1^2 + 2 \langle m_2 \cdot u \rangle l_1 \dot{\theta}_1 \dot{\theta}_2 \cos (\theta_2 - \theta_1) + \langle m_2 \cdot r^2 \rangle \dot{\theta}_2^2 \right)$$

$$PE = -m_2 l_1 g \cos \theta_1 - \langle m_2 \cdot u \rangle g \cos \theta_2$$

Thus, the Lagrangian can be represented by:

$$L = \frac{1}{2} a_{11} \dot{\theta}_1^2 + (a_{12} + b_{12} \cos (\theta_2 - \theta_1)) \dot{\theta}_1 \dot{\theta}_2 + \frac{1}{2} a_{22} \dot{\theta}_2^2 + c_1 \cos \theta_1 + c_2 \cos \theta_2$$

where:

$$a_{11} = 2 \langle m_1 \cdot r^2 \rangle + 4 \langle m_b \cdot r^2 \rangle_{++} + (m_2 + 2m_b + m_c + 2m_s + m_n) l_1^2$$

$$a_{12} = 2 \langle m_b \cdot r^2 \rangle_{-+}$$

$$a_{22} = \langle m_2 \cdot r^2 \rangle + 2 \langle m_b \cdot r^2 \rangle_{--} + \langle m_c \cdot r^2 \rangle + 2 \langle m_s \cdot r^2 \rangle + \langle m_n \cdot r^2 \rangle$$

$$b_{12} = \langle m_2 \cdot u \rangle l_1$$

$$c_1 = (2 \langle m_1 \cdot u \rangle + (m_2 + 2 m_b + m_c + 2 m_s + m_n) l_1) g$$

$$c_2 = \langle m_2 \cdot u \rangle g$$

The canonical momenta can be calculated from the Lagrangian:

$$p_1 = \frac{\partial L}{\partial \dot{\theta}_1} = a_{11} \dot{\theta}_1 + (a_{12} + b_{12} \cos(\theta_2 - \theta_1)) \dot{\theta}_2$$

$$p_2 = \frac{\partial L}{\partial \dot{\theta}_2} = (a_{12} + b_{12} \cos(\theta_2 - \theta_1)) \dot{\theta}_1 + a_{22} \dot{\theta}_2$$

The Hamiltonian is given by:

$$\begin{aligned} H &= p_1 \dot{\theta}_1 + p_2 \dot{\theta}_2 - L \\ &= \frac{1}{2} a_{11} \dot{\theta}_1^2 + (a_{12} + b_{12} \cos(\theta_2 - \theta_1)) \dot{\theta}_1 \dot{\theta}_2 + \frac{1}{2} a_{22} \dot{\theta}_2^2 - c_1 \cos \theta_1 - c_2 \cos \theta_2 \end{aligned}$$

By replacing $\dot{\theta}_i$ by p_i , one can convert the Hamiltonian into a form that depends only on θ_i and p_i .

$$\dot{\theta}_1 = \frac{a_{22} p_1 - b p_2}{a_{11} a_{22} - b^2}$$

$$\dot{\theta}_2 = \frac{-b p_1 + a_{11} p_2}{a_{11} a_{22} - b^2}$$

and

$$b \equiv a_{12} + b_{12} \cos(\theta_2 - \theta_1)$$

Thus:

$$H = \frac{1}{2} \frac{a_{22} p_1^2 - 2(a_{12} + b_{12} \cos(\theta_2 - \theta_1)) p_1 p_2 + a_{11} p_2^2}{a_{11} a_{22} - (a_{12} + b_{12} \cos(\theta_2 - \theta_1))^2} - c_1 \cos \theta_1 - c_2 \cos \theta_2$$

The coupled equations of motion follow:

$$\dot{\theta}_1 = \frac{\partial H}{\partial p_1} = \frac{a_{22}p_1 - (a_{12} + b_{12} \cos(\theta_2 - \theta_1))p_2}{a_{11}a_{22} - (a_{12} + b_{12} \cos(\theta_2 - \theta_1))^2}$$

$$\dot{\theta}_2 = \frac{\partial H}{\partial p_2} = \frac{-(a_{12} + b_{12} \cos(\theta_2 - \theta_1))p_1 + a_{11}p_2}{a_{11}a_{22} - (a_{12} + b_{12} \cos(\theta_2 - \theta_1))^2}$$

$$\dot{p}_1 = -\frac{\partial H}{\partial \theta_1} = -c_1 \sin \theta_1 + q(\theta_1, \theta_2, p_1, p_2)$$

$$\dot{p}_2 = -\frac{\partial H}{\partial \theta_2} = -c_2 \sin \theta_2 - q(\theta_1, \theta_2, p_1, p_2)$$

$$q(\theta_1, \theta_2, p_1, p_2) = \frac{-(a_{12} + b_{12} \cos(\theta_2 - \theta_1))p_1 + a_{11}p_2}{(a_{11}a_{22} - (a_{12} + b_{12} \cos(\theta_2 - \theta_1))^2)^2} (a_{22}p_1 - (a_{12} + b_{12} \cos(\theta_2 - \theta_1))p_2) b_{12} \sin(\theta_2 - \theta_1)$$

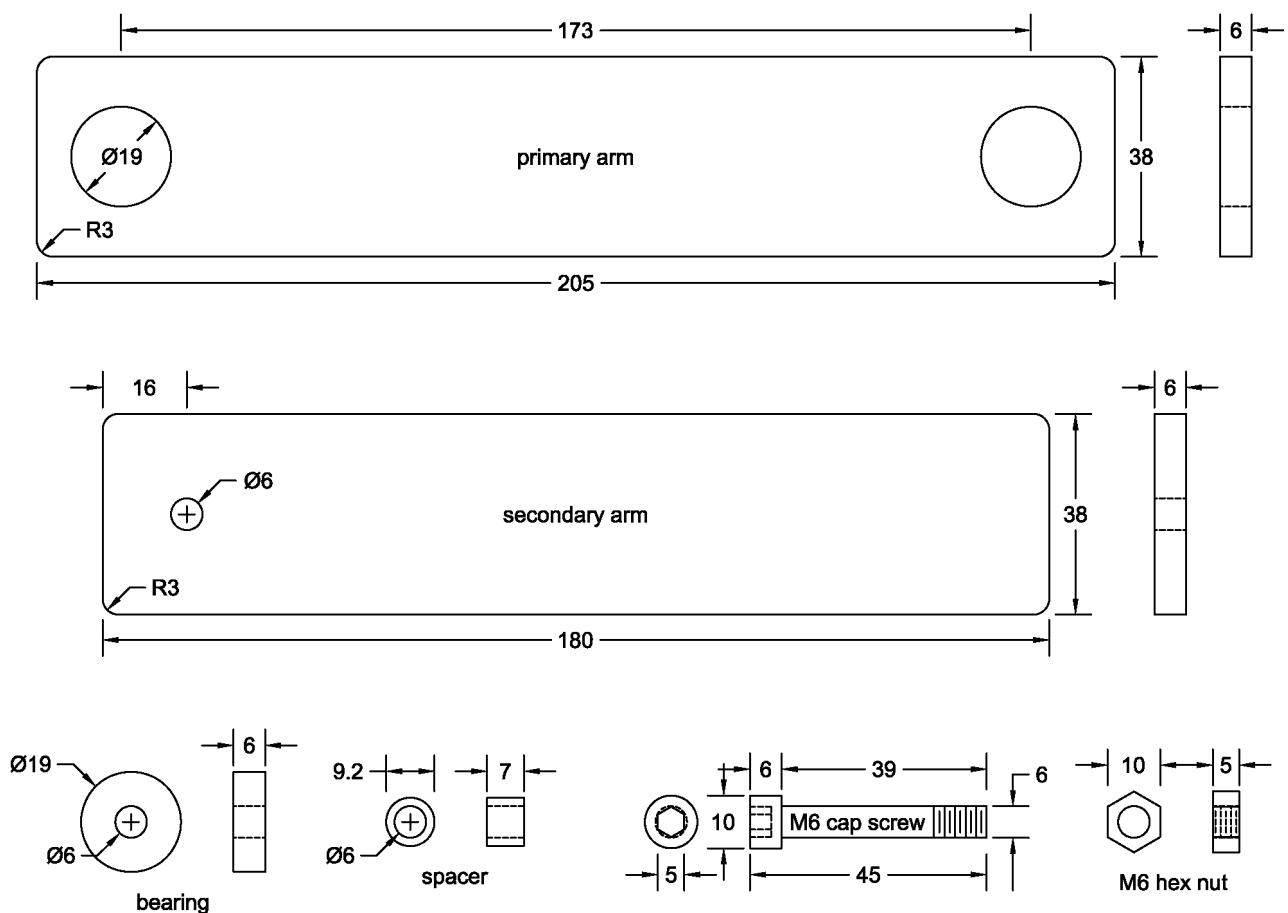


Figure 3. Double pendulum dimensions.

Dynamical stability and Lyapunov exponents

In this experiment, we would like to explore how sensitively the dynamical evolution of a system depends on the initial conditions. Do small perturbations lead to small variations or huge ones? As a starting point, consider a one-dimensional system whose evolution is governed by:

$$\dot{q} = f(q(t))$$

Suppose we want to find out how q will evolve for slightly different initial conditions in the neighborhood of q_0 :

$$\Delta\dot{q} = f(q(t)) - f(q_0(t)) \approx \frac{\partial f}{\partial q} \Delta q$$

Thus, in the limit, $\Delta q \rightarrow 0$,

$$\left. \frac{\Delta\dot{q}}{\Delta q} = \frac{\partial f}{\partial q} \right|_{q_0} \equiv \lambda \Rightarrow \Delta q(t) \approx e^{\lambda t} \Delta q(0)$$

The value, λ , is the Lyapunov exponent at q_0 . If it is greater than zero, the evolution of the system diverges exponentially with time, preventing all attempts to compute the motion at arbitrary times.

We can take this example to the next level of complexity by considering the simple pendulum. The Lagrangian for this system is:

$$L = T - V = \frac{1}{2} \langle m \cdot r^2 \rangle \dot{\theta}^2 + \langle m \cdot u \rangle g \cos \theta$$

The canonical momentum is:

$$p = \frac{\partial L}{\partial \dot{\theta}} = \langle m \cdot r^2 \rangle \dot{\theta}$$

and thus the Hamiltonian is:

$$H = p\dot{\theta} - L = \frac{p^2}{2\langle m \cdot r^2 \rangle} - \langle m \cdot u \rangle g \cos \theta$$

$$\dot{\theta} = \frac{\partial H}{\partial p} = \frac{p}{\langle m \cdot r^2 \rangle}$$

$$\dot{p} = -\frac{\partial H}{\partial \theta} = -\langle m \cdot u \rangle g \sin \theta$$

We would like to find out how the motion evolves for small perturbations from the initial condition specified by θ_0 and p_0 .

$$\Delta \dot{\theta} \cong \frac{\partial^2 H}{\partial \theta \partial p} \Delta \theta + \frac{\partial^2 H}{\partial^2 p} \Delta p = \frac{\Delta p}{\langle m \cdot r^2 \rangle}$$

$$\Delta \dot{p} \cong -\frac{\partial^2 H}{\partial^2 \theta} \Delta \theta - \frac{\partial^2 H}{\partial \theta \partial p} \Delta p = -\langle m \cdot u \rangle g \cos \theta \Delta \theta$$

This can be represented by the matrix equation below:

$$\begin{pmatrix} \Delta \dot{\theta} \\ \Delta \dot{p} \end{pmatrix} = \begin{pmatrix} 0 & \frac{1}{\langle m \cdot r^2 \rangle} \\ -\langle m \cdot u \rangle g \cos \theta & 0 \end{pmatrix} \begin{pmatrix} \Delta \theta \\ \Delta p \end{pmatrix}$$

We seek solutions of the form:

$$\begin{pmatrix} \dot{a} \\ \dot{b} \end{pmatrix} = \begin{pmatrix} m_{11} & m_{21} \\ m_{12} & m_{22} \end{pmatrix} \begin{pmatrix} a \\ b \end{pmatrix} = \lambda \begin{pmatrix} a \\ b \end{pmatrix}$$

where $\Delta q(0) \equiv a\Delta\theta + b\Delta p$ is an eigenvector for the matrix with an eigenvalue, λ , and thus $\Delta q(t) \sim e^{\lambda t} \Delta q(0)$. To find λ , the following equation must be solved:

$$\text{Det} \begin{pmatrix} m_{11} - \lambda & m_{21} \\ m_{12} & m_{22} - \lambda \end{pmatrix} = 0$$

For this particular case, the resulting equation is:

$$\lambda^2 = -g \frac{\langle m \cdot u \rangle \cos \theta}{\langle m \cdot r^2 \rangle}$$

For $\theta < \frac{\pi}{2}$, the values of λ are imaginary. However, for $\theta > \frac{\pi}{2}$, one of the values is positive and real, leading to divergent growth. The eigenvalues and eigenvectors (normal modes) are thus:

$$\theta < \frac{\pi}{2}: \quad \lambda_{\pm} = \pm i \sqrt{\frac{\langle m \cdot u \rangle g \cos \theta}{\langle m \cdot r^2 \rangle}}$$

$$e_{\pm} = \begin{bmatrix} 1 \\ \pm i \sqrt{\langle m \cdot u \rangle \langle m \cdot r^2 \rangle g \cos \theta} \end{bmatrix}$$

$$\theta \geq \frac{\pi}{2}: \quad \lambda_{\pm} = \pm \sqrt{\frac{-\langle m \cdot u \rangle g \cos \theta}{\langle m \cdot r^2 \rangle}}$$

$$e_{\pm} = \begin{bmatrix} 1 \\ \pm \sqrt{-\langle m \cdot u \rangle \langle m \cdot r^2 \rangle g \cos \theta} \end{bmatrix}$$

To understand the long term behavior of the system, one must average the Lyapunov exponents over the dynamical path in the phase space.

It is worth remarking about a generic property of Lyapunov exponents stemming from the Hamiltonian description. The Jacobian matrix that transforms the phase space volume, $\Delta\theta_1 \cdot \Delta p_1 \cdot \Delta\theta_2 \cdot \Delta p_2 \dots$ must have the form:

$$J = \begin{bmatrix} \frac{\partial^2 H}{\partial \theta_1 \partial p_1} & \frac{\partial^2 H}{\partial p_1^2} & \frac{\partial^2 H}{\partial p_1 \partial \theta_2} & \frac{\partial^2 H}{\partial p_1 \partial p_2} & \dots \\ -\frac{\partial^2 H}{\partial \theta_1^2} & -\frac{\partial^2 H}{\partial \theta_1 \partial p_1} & -\frac{\partial^2 H}{\partial \theta_2 \partial \theta_2} & -\frac{\partial^2 H}{\partial \theta_1 \partial p_2} & \dots \\ \vdots & \vdots & \vdots & \vdots & \dots \end{bmatrix}$$

The diagonal elements of this matrix cancel in pairs so that the trace of J is zero. This guarantees that the sum of eigenvalues, ie. the Lyapunov exponents, is also zero. The physical implication of this is the invariance of phase space volume for a conservative system. For a dissipative system, this would not be true.

This analysis can be extended to the double pendulum although the expressions become algebraically messy. In this case, we will only be interested in obtaining numerical solutions.

The Jacobian matrix for this problem is a 4×4 array:

$$J = \begin{bmatrix} J_{11} & J_{12} & J_{13} & J_{14} \\ J_{21} & J_{22} & J_{23} & J_{24} \\ J_{31} & J_{32} & J_{33} & J_{34} \\ J_{41} & J_{42} & J_{43} & J_{44} \end{bmatrix}$$

By defining the following intermediate quantities, the matrix elements can be computed fairly easily. (See previous parameter definitions.)

$$r \equiv a_{12} + b_{12} \cos(\theta_2 - \theta_1)$$

$$s \equiv a_{11}a_{22} - r^2$$

$$t \equiv a_{22} p_1 - r p_2$$

$$u \equiv -r p_1 + a_{11} p_2$$

$$q \equiv \frac{t u b_{12} \sin(\theta_2 - \theta_1)}{s^2}$$

$$dq = -\frac{t u b_{12} \cos(\theta_2 - \theta_1) + (t p_1 + u p_2) b_{12}^2 \sin^2(\theta_2 - \theta_1)}{s^2} + \frac{4 r t u b_{12}^2 \sin^2(\theta_2 - \theta_1)}{s^3}$$

The individual matrix elements are given by:

$$j_{11} = \frac{(s p_2 - 2 a_{22} u) b_{12} \sin(\theta_2 - \theta_1)}{s^2}$$

$$j_{12} = \frac{a_{22}}{s}$$

$$j_{13} = \frac{(s p_2 - 2 r t) b_{12} \sin(\theta_2 - \theta_1)}{s^2}$$

$$j_{14} = -\frac{r}{s}$$

$$j_{21} = -c_1 \cos \theta_1 + dq$$

$$j_{22} = -j_{11}$$

$$j_{23} = -dq$$

$$j_{24} = j_{33}$$

$$j_{31} = -j_{33}$$

$$j_{32} = j_{14}$$

$$j_{33} = \frac{(s p_1 - 2 r u) b_{12} \sin(\theta_2 - \theta_1)}{s^2}$$

$$j_{34} = \frac{a_{11}}{s}$$

$$j_{41} = j_{23}$$

$$j_{42} = -j_{13}$$

$$j_{43} = -c_2 \cos \theta_2 + dq$$

$$j_{44} = -j_{33}$$

In general, the characteristic equation defining the eigenvalues would be fourth-order in λ . The traceless nature of J requires the cubic term in λ to vanish and similar other symmetries imposed by the Hamiltonian origin squelch the linear term as well. Thus, the defining equation for the eigenvalues takes the form:

$$(\lambda^2)^2 + 2 b \lambda^2 + c = 0$$

and thus:

$$\lambda^2 = -b \pm \sqrt{b^2 - c}$$

where:

$$b = -\left(\frac{1}{2}(j_{11}^2 + j_{33}^2 + j_{12} j_{21} + j_{34} j_{43}) + j_{23} j_{32} + j_{24} j_{42}\right)$$

$$c = \text{Det } |J|$$

The values for λ^2 may be complex.

Equipment

Double pendulum: The centerpiece of this experiment is a double pendulum purchased from www.chaoticpendulums.com. (If you would like one of your own, the price was listed at \$150 plus shipping on April 2010.) The unit is fastened to a $\frac{1}{8}$ " thick steel plate 46" above the floor. The detailed mechanical parameters are listed in Table I. The steel plate provides a convenient surface for attaching a variety of magnetic base accessories for repeatedly releasing the pendulum from specific positions and recording the resulting motion. **Please use some care in placing these gadgets so they don't slam onto the enameled surface.**

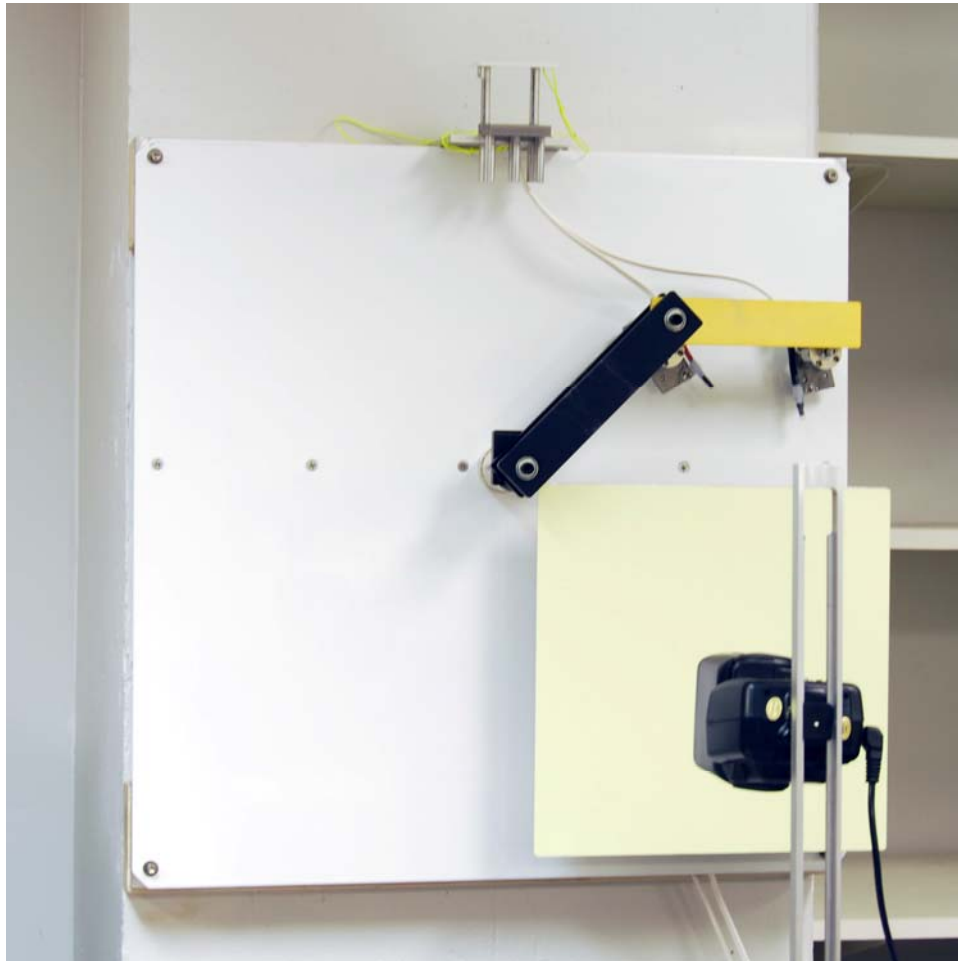


Figure 4. The double pendulum arms held at $\theta_1 = 135^\circ$, $\theta_2 = 90^\circ$ by two solenoids. The phosphorescent screen is in the lower right corner and the flash gun can be seen in the foreground.

Solenoid releases: Two solenoid assemblies are available to hold each arm of the double pendulum at a fixed predetermined location prior to release. The plungers must be pulled out manually to hold the arms. Note that the two solenoid assemblies are not quite identical – each

arm requires a specific spacing of the solenoid from the vertical steel mount plate. The power to activate the solenoids is provided by an electronics enclosure that is triggered by a timing unit.

Electronic flash gun: The angular coordinates of the double pendulum arms are captured at preset times by a short duration burst from a LumoPro LP120 manual flash unit. This device was chosen because the vendor was reasonably willing to provide information about trigger requirements. The unit is battery-powered so the appropriate switches must be turned on to activate. Set intensity switches to *NEXT* and *1/8* to optimize flash duration and brightness. **Please also make sure to switch unit off before you leave.** The LP120 takes about 10 seconds or so to charge as indicated by a small red LED near the on/off switch. If longer, swap rechargeable batteries.

Phosphorescent screen: With the bright light from the flash gun, the angular positions of the double pendulum arms can be recorded by phosphorescent screens, either 12" \times 12" or 6" \times 6" in area. This will only work in a darkened room. The image decay time is of the order of 30 seconds. This provides a reasonable opportunity to measure the shadows of the pendulum arms. In case of any need for replacements, the screen material is ZnS vinyl film and was obtained from Educational Innovations, Inc. and Hanovia Specialty Lighting.



Figure 5. The shadow image of the double pendulum caught by the electronic flash gun.

Angle gauge: An electronic Wixey digital angle gauge is available to measure the angles of the pendulum components before release and the positions indicated by the shadows on the phosphorescent screens afterwards. An aluminum and steel holder will help determine the location of the pendulum arms prior to release and a PVC plastic block will help determine the angles indicated by the shadows on the phosphorescent screens. The gauge reference angle must be initialized so that zero angle coincides with the vertical. The resolution of this device is 0.1° .

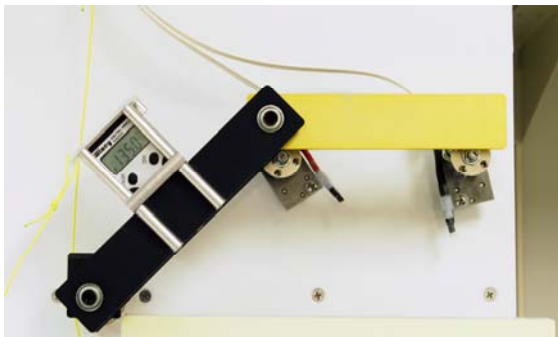


Figure 6. Measurement of the primary arm angle. (Please keep a hand on the gauge so that it doesn't accidentally fall.)

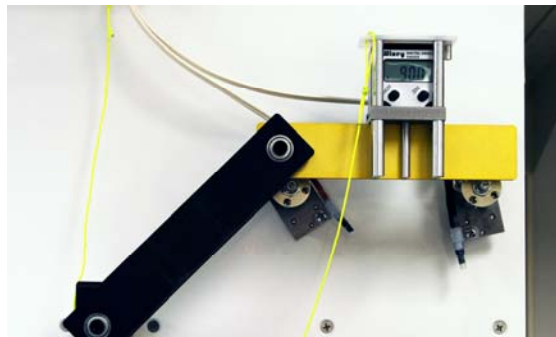


Figure 7. Measurement of the secondary arm angle. (Please keep a hand on the gauge so that it doesn't accidentally fall.)

Red flashlight: A Celestron night vision red LED flashlight is available to read the Wixey angle gauge without bleaching the phosphorescent screen image. A rotating thumbwheel turns the device on and adjusts the intensity of light. Turn off when not in use.

Photogate timing device: A Vernier photogate is available to measure the oscillation period of the double pendulum under restricted conditions. This permits some simple checks of the mechanical parameters that determine the equations of motion. A beam alignment rod should be used to help position the photogate so that the unit triggers near the zero angle point of the pendulum arm.

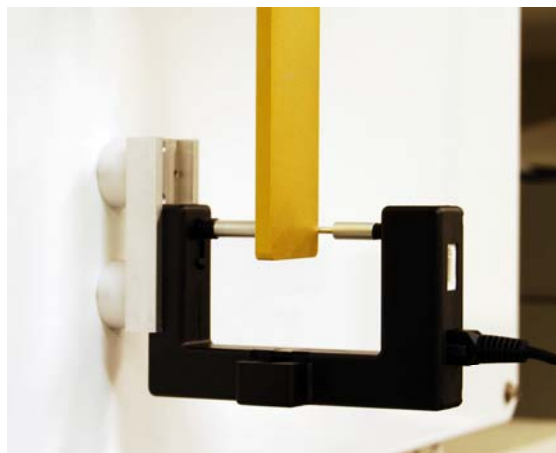


Figure 8. Use of beam alignment rod to position the Vernier photogate.

Leveling table: A small leveling table is available to help set the reference angle for the Wixey digital gauge. Adjust the three leveling screws so that the 2" diameter steel ball has no tendency

to roll in any specific direction. This should determine the level to about 0.1° . You can do slightly better by nulling the Wixey gauge at this position and then rotating the gauge by 180° around a vertical axis. If this is a true level, the gauge will continue to indicate 0° . If not, compensate by small rotations of the leveling screws. Rotate by 90° and repeat. A small steel block has been provided to set the zero reference to true vertical.



Figure 9. Leveling table with 2" diameter steel ball. Adjust screws until ball position is neutral.



Figure 10. Leveling table with steel block to set the Wixey digital angle gauge reference direction to vertical.

Timing system: An ORTEC model 871 timer and counter NIM module performs the task of controlling the timing sequence that releases the double pendulum solenoids and fires the flash gun after a preset time interval. The solenoid release is initiated by the signal labeled INTERVAL and the flash gun is triggered by END OF PRESET. Both of these signals must be connected by BNC cables to the electronic enclosure mentioned earlier. An internal clock is available to provide flash gun delays from 0.1 to 1.0 second in 0.1 second increments and from 2 to 10 seconds in 1 second increments. The module as shown in Figure 11 is set for an interval of 2 seconds. For any other delays, the timing can be determined by an external clock signal plugged into the EXT CLOCK BNC jack in the rear panel of the module and TIME BASE SELECT set to EXT. The count interval must also be set appropriately. For example, a 10 KHz external clock and a preset count of $M = 3$, $N = 4$ will generate a 3.0 second delay sequence. Press STOP, RESET and COUNT to activate the solenoids holding the pendulum arms and fire the flash lamp at the end of the preset time.



Figure 11. ORTEC timer & counter module.

External function generator: An H-P 33120A function generator should be used to furnish an external clock signal to the ORTEC 871. The waveform must be set to square wave. Set *Ampl* to 2.000 V RMS, *Offset* to 1.5 V, and *% Duty* to 20 % (To access the *% Duty* function, press the *Shift* button.). For intervals of the order of 1 second, use frequencies of the order of 25 KHz.

Double pendulum mechanical parameters

| <i>Parameter</i> | <i>Value</i> | <i>Units</i> |
|---|----------------|--------------------|
| g | 9802.894276 | mm s ⁻² |
| l_1 | 173.000000 | mm |
| $\langle m_1 \cdot u \rangle$ | 10123.312735 | g mm |
| $\langle m_1 \cdot r^2 \rangle$ | 1262802.391807 | g mm ² |
| m_2 | 110.362483 | g |
| $\langle m_2 \cdot u \rangle$ | 8200.761340 | g mm |
| $\langle m_2 \cdot r^2 \rangle$ | 919788.854796 | g mm ² |
| m_b | 7.369667 | g |
| $\langle m_b \cdot r^2 \rangle_{--}$ | 48.200077 | g mm ² |
| $\langle m_b \cdot r^2 \rangle_{-+}$ | 55.763811 | g mm ² |
| $\langle m_b \cdot r^2 \rangle_{++}$ | 205.992010 | g mm ² |
| m_s | 2.014000 | g |
| $\langle m_s \cdot r^2 \rangle$ | 30.371120 | g mm ² |
| m_c | 3.704000 | g |
| $\langle m_c \cdot r^2 \rangle$ | 27.089327 | g mm ² |
| m_n | 0.291000 | g |
| $\langle m_n \cdot r^2 \rangle$ | 5.366072 | g mm ² |
| Table I. Kinematic parameters for the double pendulum. These values may be cut and pasted from the file, <i>pendulum_params.xls</i> . | | |

Validation tests

The physical parameters for the double pendulum used in this experiment are listed in Table I. The various mass moments were computed analytically from the relevant dimensions. To check whether these values adequately describe the system, one can constrain the two pendulum arms in various ways and accurately measure the small amplitude periods. These correspond to the following configurations:

- a. Hold the primary arm fixed and measure the oscillation frequency of the secondary arm.

$$\omega_a^2 = \frac{c_2}{a_{22}}$$

- b. Hold the secondary arm fixed inside the primary arm using a #8 elastic band near the primary axis.

$$\omega_b^2 = \frac{c_1 - c_2}{a_{11} + 2(a_{12} - b_{12}) + a_{22}}$$

- c. Hold the secondary arm fixed to and extended beyond the primary arm using two #8 elastic bands and a small rectangle of box board as a stiffener.

$$\omega_c^2 = \frac{c_1 + c_2}{a_{11} + 2(a_{12} + b_{12}) + a_{22}}$$

The periods and thus the oscillation frequencies can be accurately measured with a Vernier photogate interfaced to the computer.



Figure 12. Pendulum period test configuration (a).



Figure 13. Pendulum period test configuration (b).



Figure 14. Pendulum period test configuration (c).

Numerical simulation of the double pendulum

The previous measurements should validate the pendulum parameters to the accuracy of the order of 0.1%. The next step is to use these values to predict the pendulum behavior over a finite range of time of the order of 10 seconds. The most convenient numerical technique is Runge-

Kutta integration. The input is a 4-vector of initial conditions, $(\theta_1, p_1, \theta_2, p_2)$ and a vector set of functions that predict the first-order time derivative of each dynamic variable as a function of these four quantities. Use time steps of the order of 0.001 s to ensure accurate estimations.

I have used the IDL numerical analysis package to compute and plot the behavior of this double pendulum system as depicted in Figures 15, 16, and 17. This requires two or three dozen lines of code. I expect that most students are more likely to have experience with MatLab. Program scripts for both IDL and MatLab are available on the Physics 441/442 Web site. For IDL, you will need *d_chaos.pro*, *d_pend.pro* and *lyapunov.pro*. MatLab requires *d_chaos.m*, *d_pend.m*, *lyapunov.m* and *rk4.m* (The last file performs Runge-Kutta integration. This code is already embedded in IDL.) In the course of this experiment, you will be required to perform additional calculations to explore the chaotic motion but these routines should be a useful starting point.

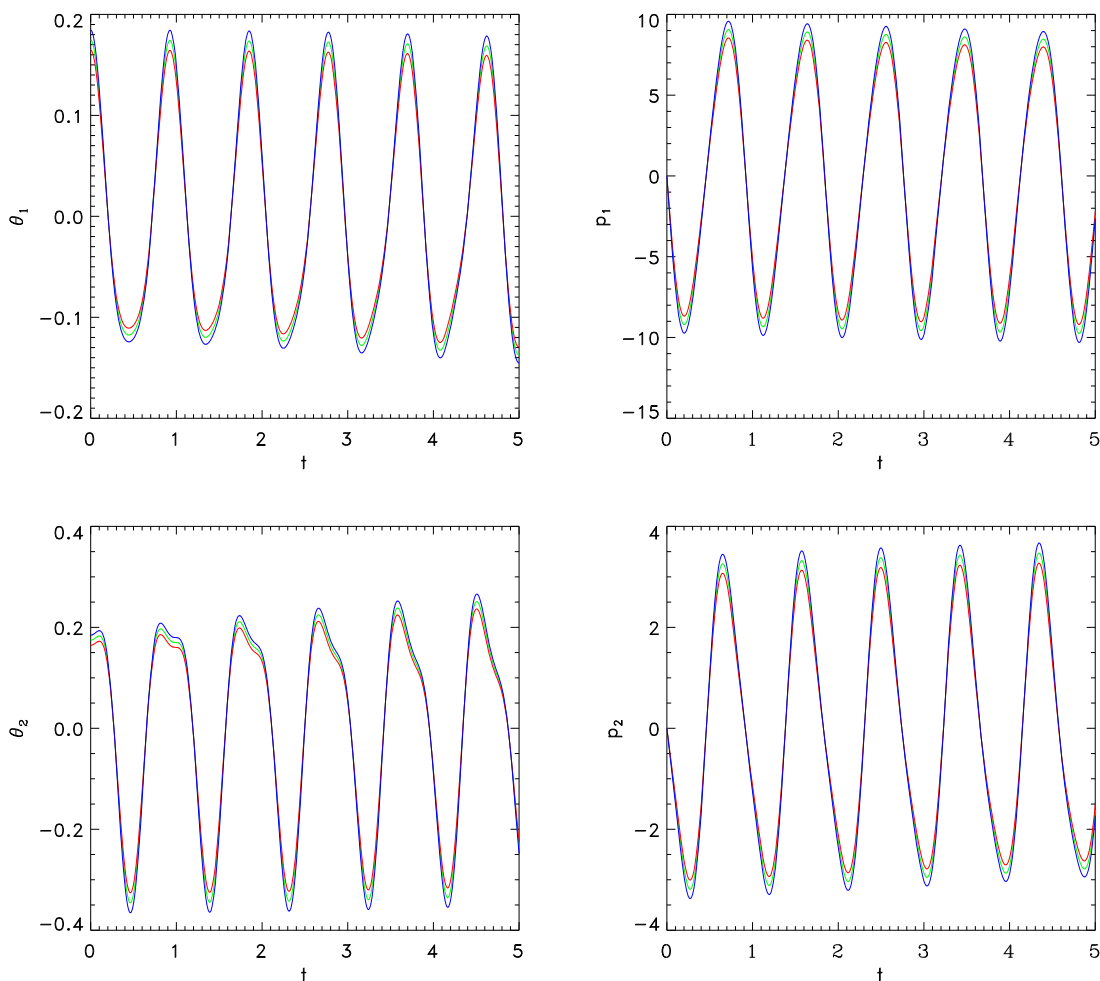


Figure 15. Graphs of $\theta_1(t)$, $p_1(t)$, $\theta_2(t)$, $p_2(t)$ for $\theta_1(0) = 10^\circ$, $\theta_2(0) = 10^\circ$. The red, green and blue lines show the behavior for three initial conditions for θ_1 and θ_2 that vary by 0.01 radians.

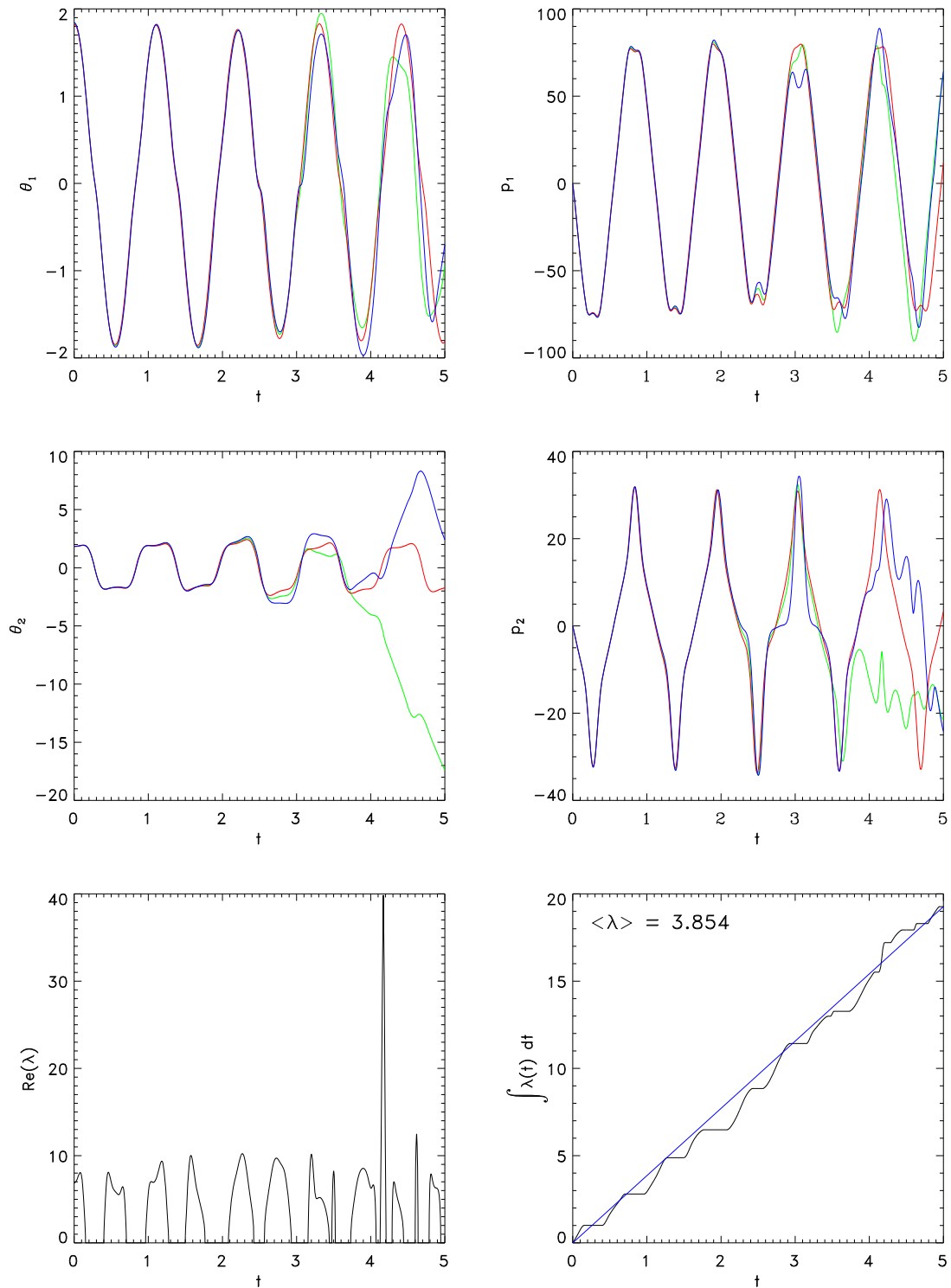


Figure 16. Graphs of $\theta_1(t)$, $p_1(t)$, $\theta_2(t)$, $p_2(t)$ for $\theta_1(0) = 105^\circ$, $\theta_2(0) = 105^\circ$. The red, green and blue lines show the behavior for three initial conditions for θ_1 and θ_2 that vary by 0.01 radians. The lower two graphs show the Lyapunov exponent along the central trajectory.

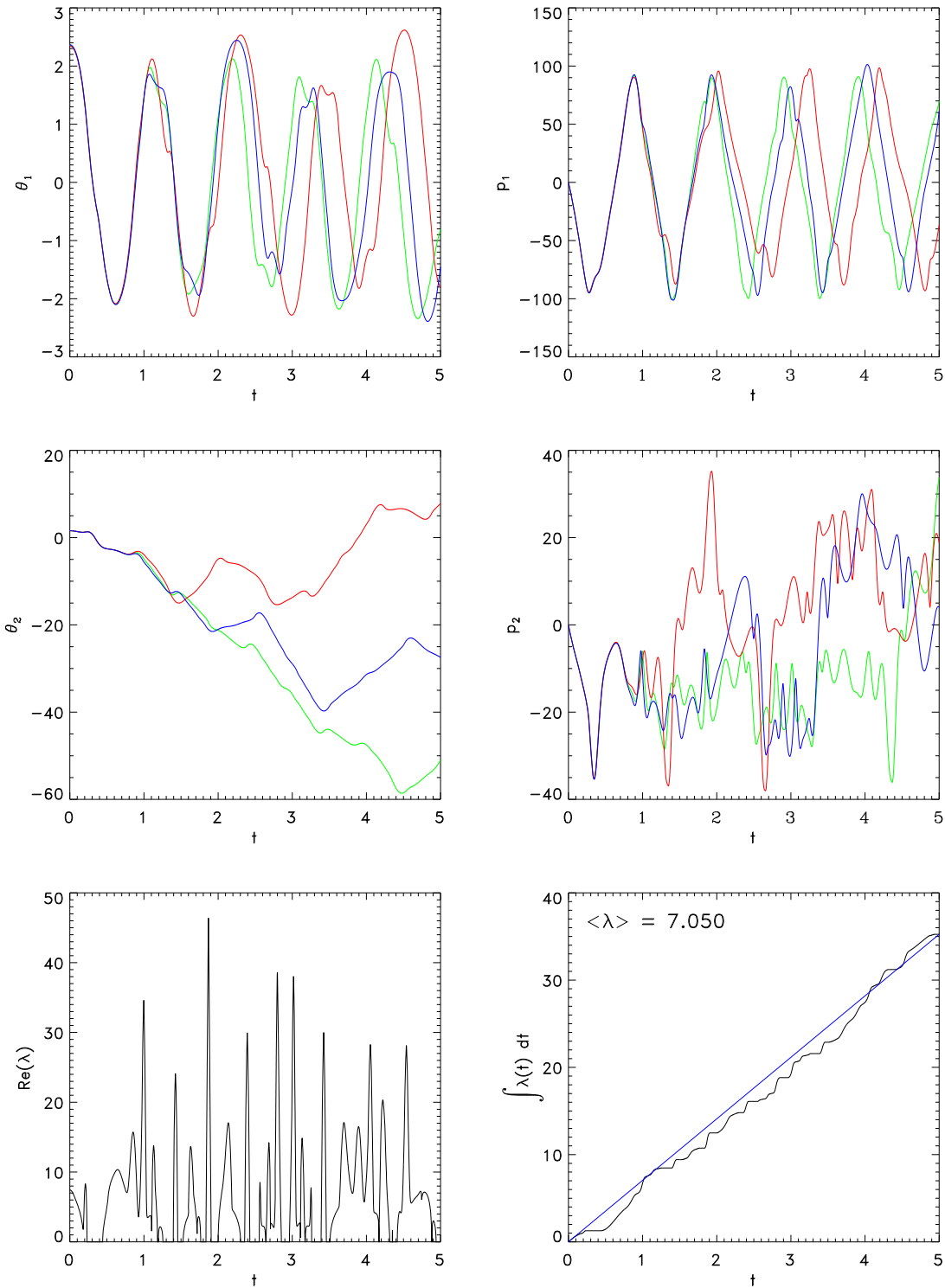


Figure 17. Graphs of $\theta_1(t)$, $p_1(t)$, $\theta_2(t)$, $p_2(t)$ for $\theta_1(0) = 135^\circ$, $\theta_2(0) = 90^\circ$. The red, green and blue lines show the behavior for three initial conditions for θ_1 and θ_2 that vary by 0.01 radians. The lower two graphs show the Lyapunov exponent along the central trajectory.

Experimental observations

The main goal of this experiment is to examine the behavior of the double pendulum as a function of initial conditions using both computational and experimental techniques. A useful set of initial conditions to explore is $(\theta_1 = n\pi/12, p_1 = 0, \theta_2 = n\pi/12, p_2 = 0)$ where n is an integer in the range from 3 to 9. For small values of n , the experimentally measured pendulum positions will track the calculations accurately and the dispersion of values at fixed time will be small. As n gets larger, the differences between the measured and computed displacements will grow, followed by increases in the dispersions at fixed times. The technique for these measurements is to set up the electronic flash lamp to trigger at the desired time delay after solenoid release and then immediately place the Wixey angle gauge and block on the phosphorescent screen to read off the pendulum arm positions at the time of flash. (See Figures 18 & 19 below.) To determine dispersion, measure θ_1 and θ_2 for ten identical releases from the same initial conditions and compute the standard deviation. You need to be aware that for large values of n , the secondary pendulum arm can easily have executed one more or one less complete rotation, making dispersion estimates unreliable under these conditions. For motion in the chaotic regime, plot the log of dispersion as a function of time.

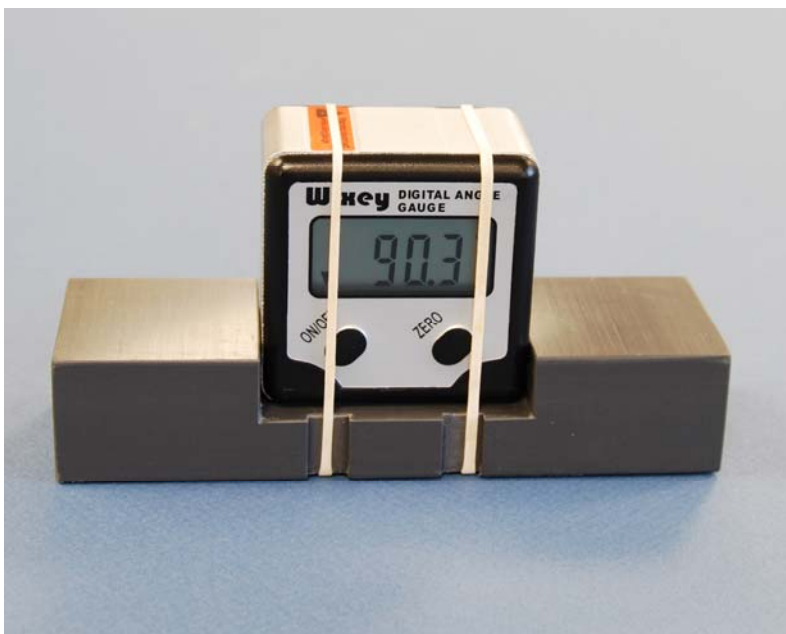


Figure 18a. Wixey digital angle gauge and retainer block for measuring shadow angles on the phosphorescent screen.

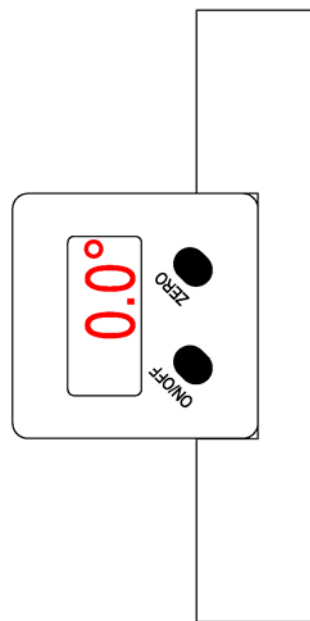


Figure 18b. Angle gauge zero reference position.

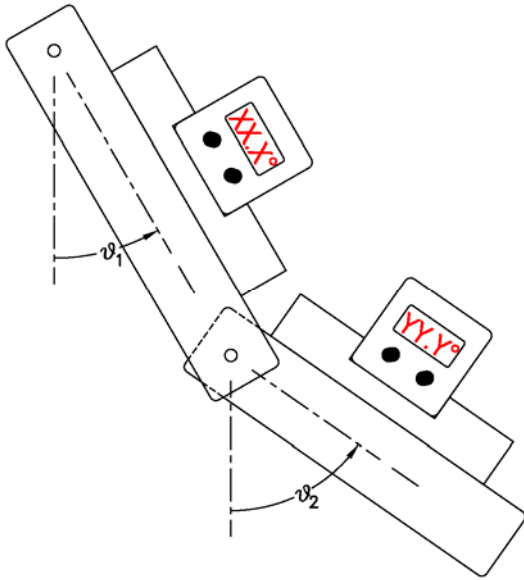


Figure 19a. If the digital gauge is to the right of the corresponding axis:
 $\theta_1 = 180^\circ - XX.X$; $\theta_2 = 180^\circ - YY.Y$.

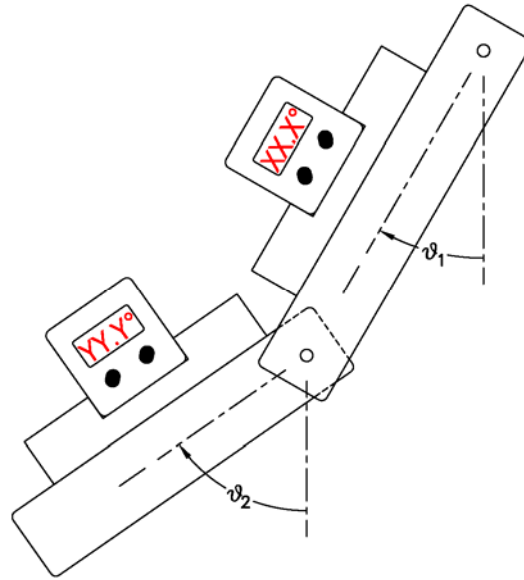


Figure 19b. If the digital gauge is to the left of the corresponding axis:
 $\theta_1 = - XX.X$; $\theta_2 = - YY.Y$.

The dispersion of phase space trajectories should be simultaneously explored with numerical techniques. Vary a particular initial condition for $(\theta_1, p_1, \theta_2, p_2)$ by $(\delta\theta_1, 0, \delta\theta_2, 0)$ where $\delta\theta_1$ and $\delta\theta_2$ are Gaussian distributed random errors with standard deviations of the order of 0.0005 radians. If you only have access to a uniform random number generator over the interval, $[0 \leq r \leq 1]$, use $r_{Gauss} = r_1 + r_2 + \dots + r_{11} + r_{12} - 6$. Generate a hundred or so trajectories to compute the dispersion. Compare these results qualitatively with the corresponding experimental measurements.

I noted that the experimentally measured dispersions were not always very stable in value, even if the mean positions were quite reproducible. That may be an artifact of the strong possibility that Gaussian initial errors do not propagate to Gaussian trajectory dispersions. This is an open question for the moment that could be explored by computational methods.

Relation to Fractals and Other Complex Behavior

Although the double pendulum does not give rise to interesting geometric behavior, the general computational procedure often produces surprising results. The figure below was taken from a recent New York Times Web blog by Steven Strogatz. The image depicts the behavior of Newton's method for iteratively computing the solution to $z^3 = 1$. The color of each point in the figure indicates which of the three roots will be approached from that particular point in the complex plane.

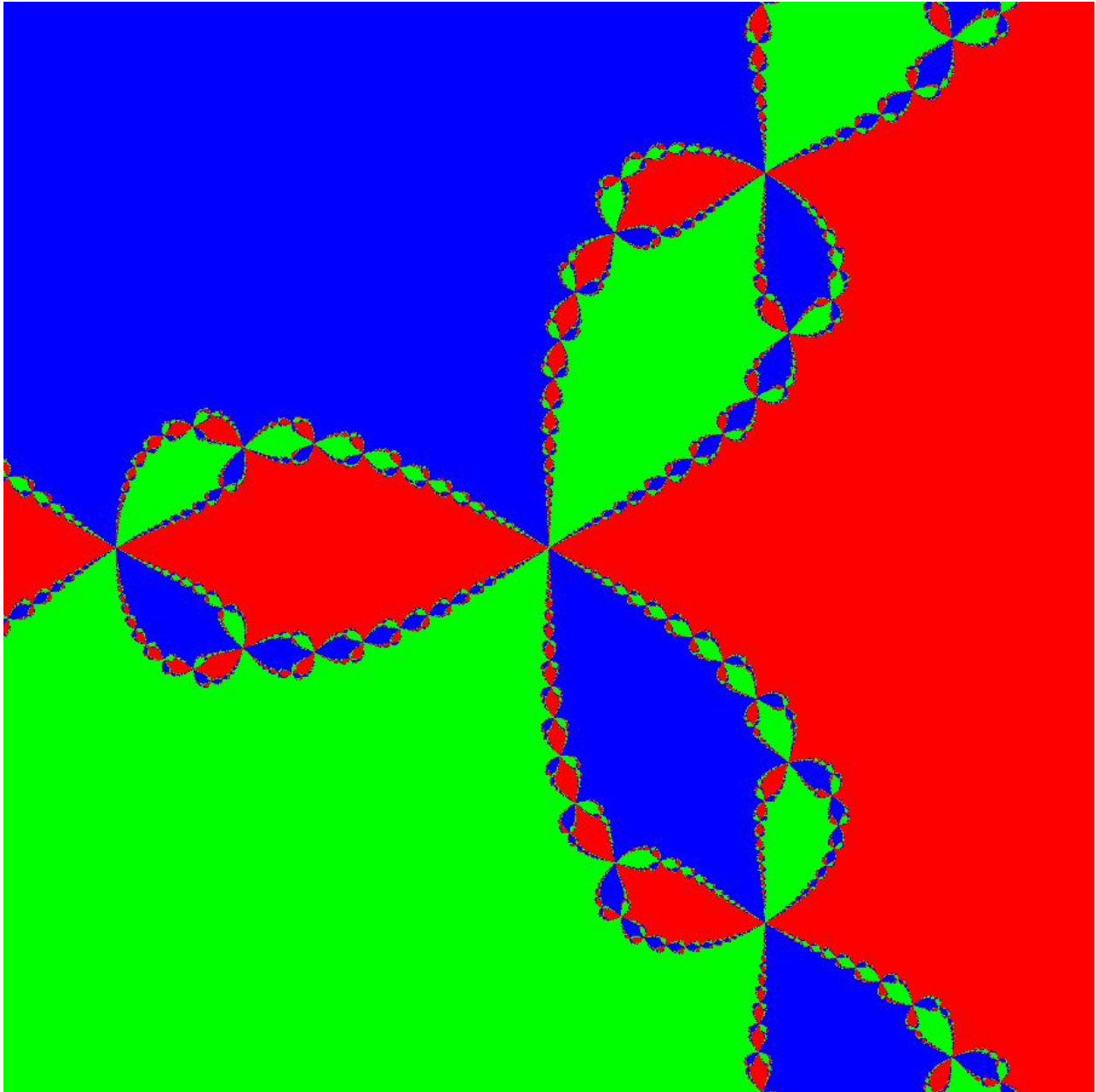


Figure 20. A map of the complex plane with $-1 \leq \text{Re}(z) \leq 1$ and $-1 \leq \text{Im}(z) \leq 1$. The three colors designate which complex root will be found by iteration of Newton's method for the solution of $z^3 = 1$. See S. Strogatz.

Useful mathematical formulas:

$$\int_0^a \int_0^b (x^2 + y^2) dx dy = \frac{1}{3}(a^2 + b^2)ab$$

$$\int_0^r dx \int_0^{\sqrt{r^2-x^2}} ((x_0+x)^2 + (y_0+y)^2) dy = \frac{r^2}{24} (16(x_0+y_0)r + 3\pi(r^2 + 2(x_0^2 + y_0^2)))$$

$$\sqrt{a+bi} = \pm(c+di) \quad ; \quad d = \frac{\sqrt{-a+\sqrt{a^2+b^2}}}{\sqrt{2}}, \quad c = \frac{b}{2d}$$

References

1. Troy Shinbrot, Celso Grebogi, Jack Wisdom and James A. Yorke, *Chaos in a double pendulum*, Am. J. Phys. 60, 491-499 (1992).
2. Tomasz Stachowiak and Toshio Okada, *A numerical analysis of chaos in the double pendulum*, Chaos, Solitons and Fractals **29**, 417–422 (2006).
3. Steven Strogatz, *Finding Your Roots*, New York Times, March 7, 2010.